JOURNAL OF OPTOELECTRONICS AND ADVANCED MATERIALS Vol. 11, No. 3, March 2009, p. 215 - 228

Review Paper

Advanced electrical characterization of ferroelectric thin films: facts and artifacts

L. PINTILIE
National Institute of Materials Physics, Atomistilor 105bis P.O. Box MG 7, Bucharest-Magurele, Ilfov, Romania

Ferroelectric materials in thin film form, largely used in a broad variety of high-tech applications, are characterized by performing electrical measurements on capacitor-like structures. A complete characterization should include hysteresis, capacitance, and current measurements performed at different bias voltages, frequencies and temperatures. The analysis of the experimental data should be made considering that the real test structure is metal-ferroelectric-metal, and taking care of the direct impact of the microstructure on the macroscopically measured quantities. Further on, the theoretical models developed to simulate the experimental results should be able to explain simultaneously the data obtained from different types of electrical measurements. The main type of electrical measurements performed on ferroelectric capacitors will be discussed in detail. A special attention will be given to some important problems such as: the electrode-ferroelectric interfaces; calculation of the dielectric constant; intrinsic-versus-extrinsic contributions to the value of the dielectric constant; fake hysteresis loops and the question "Is the presence of the hysteresis cycle solid evidence for the presence of ferroelectricity?"; non-conventional contributions to the polarization charge and their effect on the frequency dependence of the hysteresis loop; conduction mechanisms in different ferroelectric materials. Some "hot" topic will be also discussed, as for example the validity of the serial model in the case of ferroelectric multilayers, and the coexistence of ferroelectric and antiferroelectric behavior in some structures and multilayers. The presentation is supported by experimental material collected by the author in the last 7 years, especially during his extended stay at the Max Planck Institute from Halle, Germany. The author is very grateful to V. Stancu, I. Vrejoiu and K. Boldyreva for providing most part of the samples, and to M. Alexe, D. Hesse and U. Goesele for the useful discussions and funding during the stay in Halle. Part of the experimental work was made in the frame of the contract CEEX-44-DINAFER, financed by the Romanian Ministry of Education and Research.

(Received October 25, 2008; accepted March 19, 2008)

Keywords: Ferroelectric films, Hysteresis, Capacitance, Current, Electrode interface

1. Introduction

Ferroelectric materials are intensively studied all over the world due to their unique set of properties: reversible polarization, high dielectric constant, birefringence, piezoelectricity, pyroelectricity, etc. They are widely used in a large variety of applications both in bulk form and as thin films [1,2]. The study of ferroelectric thin films was especially boosted in the last 20 years by two main factors: the continuous reduction in size of electronic components correlated with the necessity to integrate the ferroelectric materials into the semiconductor industry; the development of the new deposition techniques, such as pulsed laser deposition (PLD), allowing the growth of epitaxial films from oxide materials [3].

Ferroelectric thin films are mainly studied for non-volatile memories, but they can be used also for other applications such as actuators, pyroelectric detectors, non-linear optoelectronic components, tunable capacitors, etc [4-10]. In the vast majority of cases the ferroelectric materials are used as capacitors. The standard characterization of ferroelectric materials in thin film form is based on three types of measurements:

1. ***Capacitance measurements.*** The capacitance value measured at zero bias and at a well defined frequency (usually 1 kHz) is used to calculate the dielectric constant. The capacitance-temperature (C-T) measurement is used to extract information about the phase transition, the capacitance-voltage (C-V) measurement is used to extract information regarding the tunability, and the capacitance-frequency (C-f) measurement serves to collect data regarding the relaxation mechanisms. The basic tool for capacitance measurements is the capacitance bridge.
2. ***Hysteresis measurement.*** The hysteresis loop is considered the fingerprint for the presence of ferroelectricity. It serves to extract information about remnant polarization, coercive field, saturation polarization and switching kinetics. The basic tool for hysteresis measurements is the Sawyer-Tower circuit.
3. ***Current measurements.*** The current-voltage (I-V) characteristic obtained at different temperatures is then used to extract information regarding the conduction mechanisms responsible for the leakage current in ferroelectric thin film capacitors. The current measurements are usually performed with the aid of an electrometer or picoampermeter.

Many authors are performing only one type of measurements, eventually two, and then start building theoretical models to explain or simulate the results. Often,

these models are not fitting the other types of measurements. Therefore, one sided explanation of the electrical data is not recommended. Any theoretical model should be able to explain and simulate the electrical properties in their integrality. This means that a model developed to explain the I-V characteristic should be able to simulate the C-V and hysteresis data as well. Another aspect which is overseen when analyzing the data of the electrical measurements is that the measured structure is a capacitor, more precisely a metal-ferroelectric-metal (MFM) structure. Very little information is known about the metal-ferroelectric interface, although it can have a decisive impact on the macroscopic measurements in case of thin films [11-13]. The presence or the absence of an interface layer, whatever or not with voltage dependent properties, may have a significant impact on capacitance and current measurements. Therefore, the a-priori consideration of ohmic contacts is not recommended. The lack of knowledge regarding the properties of the metal-ferroelectric interface is responsible for some controversies such as the question if the ferroelectric layers are partly or fully depleted, or if the dielectric constant is thickness dependent [14,15].

Another aspect which is often neglected is the microstructure. The electric measurements are performed on thin films with various structure qualities, standing from nearly amorphous to high quality epitaxial. It is not recommended to compare the properties of films with different microstructures. For example, the polarization switching kinetic, the conduction mechanisms and the dielectric properties are expected to be very different in polycrystalline films compared to epitaxial ones. This fact raises the question of the intrinsic-extrinsic balance in ferroelectric thin films. Analyzing the literature it can be observed that the intrinsic properties of the most studied ferroelectric thin films, such as lead zirconate-titanate (PZT), are not really known. The values reported for the dielectric constant span from 80 to 1000, and for the polarization from 10 to 100 $\mu C/cm^2$. This fact makes difficult any simulation based on a certain model because there is a large arbitrary in selecting the numbers for the physical quantities [16-20].

Other prejudice often encountered in the field of ferroelectric materials is related to the fact that a large leakage current is incompatible with a large value of polarization. Therefore, a large effort is made to make these materials as insulating as possible. However, it can be easily observed from literature that the films with low leakage current are showing also slim hysteresis loops with low values of polarization. It is true that a large leakage current may hidden the displacive current associated to polarization reversal but, on the other hand, the absence of internal compensation charges and the structural defects making the film "insulating" through trapping and scattering of the charge carriers will affect the polarization switching kinetic also. Internal electric fields may develop, leading to back-switching phenomena concretized into a slim hysteresis and a low remnant polarization. It was theoretically shown that, to observe the polarization switching it is not obligatory to have an insulating layer, but to have high resistance interfaces with the electrodes [21]. Therefore, it is recommended to adjust the microstructure and the electrode interface properties in such a way to find an optimum between leakage and polarization, with a hysteresis loop close to rectangular.

Finally, there is the custom to translate theoretical models from one type of ferroelectric material to another, neglecting the fact that the origin of ferroelectricity may not be the same. It is true that the thermodynamic theory was very successful in explaining the basic properties of ferroelectrics, but it cannot explain the specific differences between materials with very similar crystalline structures [22]. The basic example are $PbTiO_3$ and $BaTiO_3$ or, more generally, the PZT type and $(Ba,Sr)TiO_3$ (BST) type materials. Both have the same perovskite structure, but their properties are very different. The PZT's show larger transition temperature, larger polarization and larger leakage current compared to BST's, while BST's have larger dielectric constant. These differences may be related to the fact that in $PbTiO_3$ the A-site atom, in this case Pb, has an active role in the stabilization of the ferroelectric phase through the hybridization of the Pb-O bond, while in $BaTiO_3$ the Ba-O bond is purely ionic [23].

It results that the analysis of the experimental data, in the case of ferroelectric thin films, requires some cautions and should be made carefully. Even for the same composition, the results may be very different if the microstructure is different. For this reason, models can be developed only for the tested structure and their extension to other samples may not work.

Further on the author will present some considerations regarding the basic electrical measurements and will show the cautions that should be take when analyzing the experimental data. Specific examples will be given, based on the extensive measurements performed on ferroelectric thin films with perovskite structure prepared by sol-gel or PLD, and having various microstructures. The main purpose of the article is to show that any detail counts and that unexpected results are possible.

2. Electrical measurements

2.1 Capacitance

As mentioned above, the capacitance measured at zero bias and fixe frequency is used to calculate the dielectric constant according to the equation:

$$C_m = \frac{\varepsilon_0 \varepsilon A}{d} \quad (1)$$

The notations are: C_m-measured capacitance; A-electrode area; d-layer thickness; ε_0-the permittivity of vacuum; ε-the dielectric constant.

It is clear that the application of this equation to calculate the dielectric constant disregards any detail related to microstructure (charge defects, grain boundaries, interfaces, domain walls). The obtained values is including all the intrinsic and extrinsic contributions from the MFM structure to the dielectric constant, thus cannot be ascertained as a "material constant" universally applicable to any sample of the same composition. To exemplify this fact the C-V characteristics for two PZT samples of the

same composition are shown in Fig 1, together with the photographs presenting their microstructures.

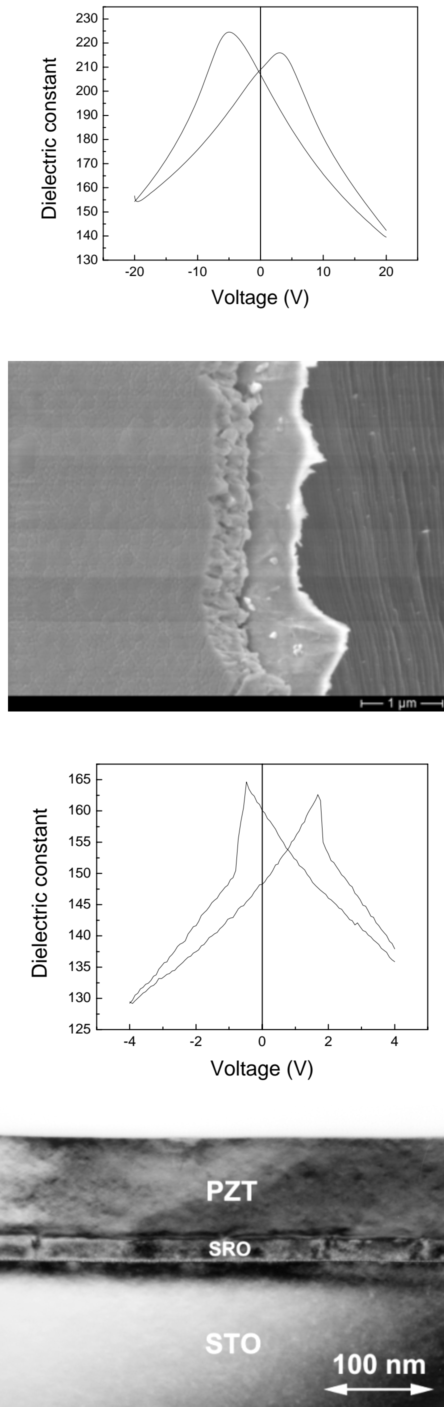

Fig. 1. Upper row: the ε-V characteristic and the scanning electron microscope (SEM) image for a polycrystalline PZT film with Zr/Ti ratio of 20/80; Lower row: the ε-V characteristic and the transmission electron microscope (TEM) image for an epitaxial film of the same composition.

As can be seen, the values of the dielectric constants are different, as well as the shape of the voltage dependence of the dielectric constant, although the composition was the same. Surely this is an effect of the microstructure. In the case of the polycrystalline film the grain boundaries are bringing and extrinsic additive contribution to the dielectric constant, leading to larger values at any bias. It means that the value obtained in the case of the epitaxial film is closer to the intrinsic one, but still can be affected by structural defects (point defects like vacancies or impurities, dislocations) and domain walls. Dislocations and domain walls can be eliminated by careful growth and by making the films thinner than the critical thickness for their formation [24-26]. Therefore, the dielectric constant should decrease as decreasing the thickness and the extrinsic contributions are eliminated in case of epitaxial films. Efforts were made to grow a batch of PZT films of the same epitaxial quality (free of dislocations and domain walls) but of different thicknesses. The thickness dependence of the dielectric constant is shown in Fig. 2.

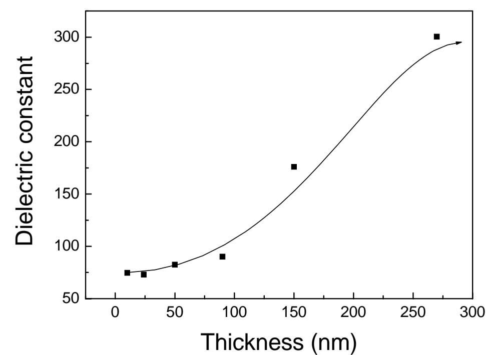

Fig. 2 The thickness dependence of the dielectric constant in the case of a batch of epitaxial PZT films with Zr/Ti ratio of 20/80.

Fig. 2 suggests that the intrinsic value of the dielectric constant in case of the PZT20/80 should be around 70. It worth notice that the theoretical values predicted for the dielectric constant of $PbTiO_3$ are in the 30-40 range [27]. The difference can be attributed to charged point defects, bringing an additive extrinsic contribution to the value of the dielectric constant. The increase with thickness appears to be an extrinsic phenomena, related to the presence of the electrode interface, which is the only extended structural defect that is present in the studied samples.

It is already accepted that the usual materials with metallic conduction used as electrodes for the ferroelectric films with perovskite structure, namely Pt and $SrRuO_3$ (SRO), are forming some potential barriers with the PZT. Therefore, the metal-PZT interface resembles in this case a typical metal-semiconductor Schottky contact [28-33]. Question is if any voltage-dependent depletion layer is developing in the present case. The presence of such a

layer implies the presence of a voltage-dependent capacitance at the electrode interface, with impact on the measured capacitance and on the thickness dependence of the "dielectric constant" calculated according to equation (1).

The presence of this voltage-dependent, Schottky type capacitance in the case of PZT-based MFM structures can be decided through the parallel analysis of the hysteresis loops and C-V characteristics [34]. This is shown in Fig. 3.

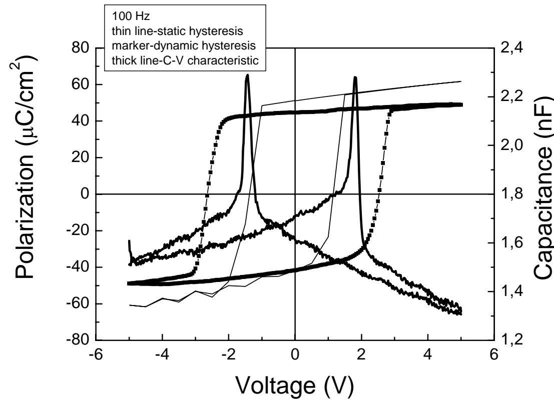

Fig. 3 The dynamic and static hysteresis loops, together with the C-V characteristic in the case of an epitaxial PZT20/80 film.

The analysis of figure 3 is based on the following relation, connecting the electric displacement D, the electric field E and the ferroelectric spontaneous polarization P_S:

$$D = \varepsilon_0 \varepsilon E + P_S \qquad (2)$$

Equation (2) says that, when P_S is saturated, then D should increase linearly with the electric field E. This is clearly seen in figure 3, especially in the static hysteresis. In this voltage range the dielectric constant ε should be voltage-independent, thus the capacitance should be constant. The C-V characteristic shows that this is not the case. It can be concluded that some voltage-dependent capacitance exists in the studied MFM structure, most probably related with the presence of Schottky type contacts at the electrode-PZT interface. Therefore, using an equivalent circuit that includes a Schottky capacitance it was possible to simulate both the frequency and voltage dependence of the capacitance in case of epitaxial films, and was shown that the thickness dependence is an extrinsic artifact. The experimental and simulated C-V characteristics are shown in figure 4a, and the simulated thickness dependence in Fig. 4b.

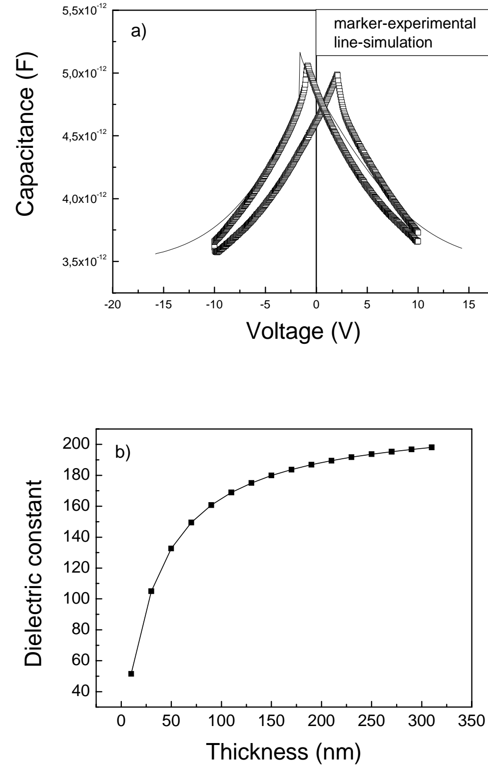

Fig. 4 a) the experimental and simulated C-V characteristics; b) the thickness dependence of the dielectric constant in case of an epitaxial PZT film.

As a conclusion for the capacitance measurements it can be said that the intrinsic value for the dielectric constant may be lower than expected, and that in the majority of cases the measured capacitance is dominated by extrinsic contributions leading to large values for the "dielectric constant" calculated with equation (1).

2.2 Hysteresis

The hysteresis loop is obtained by integrating the current flowing through the MFM structure. The real current density and the corresponding integrated charge are given by:

$$j(V) = j_l(V) + j_{tr}(V) + \frac{\partial D(V)}{\partial t}$$
$$Q(V) = \int j_l(V)dt + \int j_{tr}(V)dt + D(V) \qquad (3)$$

J_l stands for the leakage current and j_{tr} for the emission current from the traps. Ideally, these components should be zero. However, in real samples the leakage current is not zero and can reach considerable values. On the other hand, the real layers contain structural defects acting as trapping centers. This fact leads to a non-zero contribution of current from the charge carriers released

from the trapping centers. Both of these parasitic contributions add to the displacive current, producing changes in the shape of the hysteresis loop.

It is known already that the leakage current may inflate the hysteresis loop, thus this aspect will be no further discussed. I will give more attention to the traps, but first I will draw the attention that the shape of the hysteresis loop, and polarization values, are also affected by the microstructure, similar to the C-V characteristic. Figure 5 is showing the recorded loops for two samples of the same composition, PZT40/60, but with different quality of the crystalline structure.

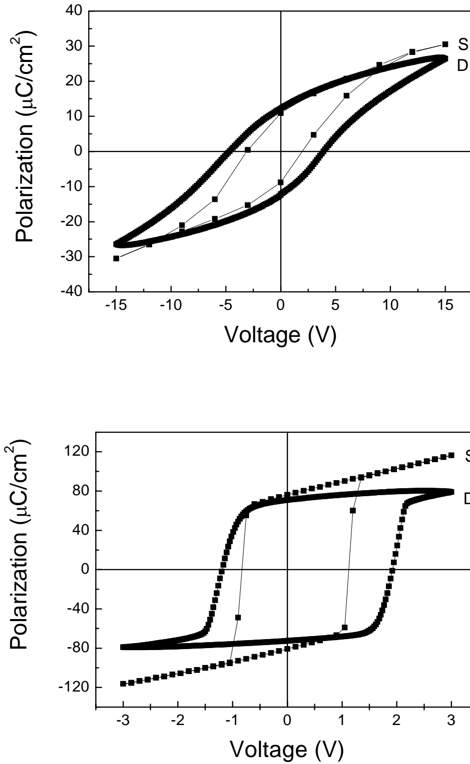

Fig. 5 Left: dynamic and static hysteresis loops for polycrystalline PZT40/60; Right: dynamic and static hysteresis loops for epitaxial PZT40/60. S is for static and D for dynamic.

The polarization value is lower in the polycrystalline film and the loop is more elongated compared to the epitaxial layer, where the polarization value is maximum compared to theoretical predictions, and the shape is almost rectangular. The difference is mainly due to the structural defects affecting the polarization switching and acting as pinning centers for the ferroelectric domains, especially the grain boundaries. When the layer is of single crystal quality, then the switching is abrupt because the domain walls can move very fast trough the film volume. In the polycrystalline film, the domain wall movement is hindered by the extended structural defects, thus the switching is more likely gradual, over a large voltage interval.

Returning to the traps, these can influence the hysteresis loop in the voltage range where the polarization is saturated. The emission current from the traps located in a depletion region of width w is given by (it was assumed that the contacts are Schottky type as suggested by the capacitance measurements in section 2.1) [35,36]:

$$I_{tr} = qA\int_0^{w_t} \frac{dn}{dt}dx \qquad \frac{dn}{dt} = -\frac{N_T(t)}{\tau} \tag{4}$$

Here, N_T is the density of the traps, τ is the emission time constant from the trap, and t is time. N_T is given by:

$$N_T(t) = N_{T0}\exp\left(-\frac{t}{\tau}\right) \tag{5}$$

For a triangular shape of the voltage used for the hysteresis measurement it can be shown that the total integrated charge, in the absence of the leakage current, is given by:

$$Q_s(V) = \left(\varepsilon_0\varepsilon + \frac{qdw_tN_{T0}}{4\tau V_a f}\right)E + P_S(V) \tag{6}$$

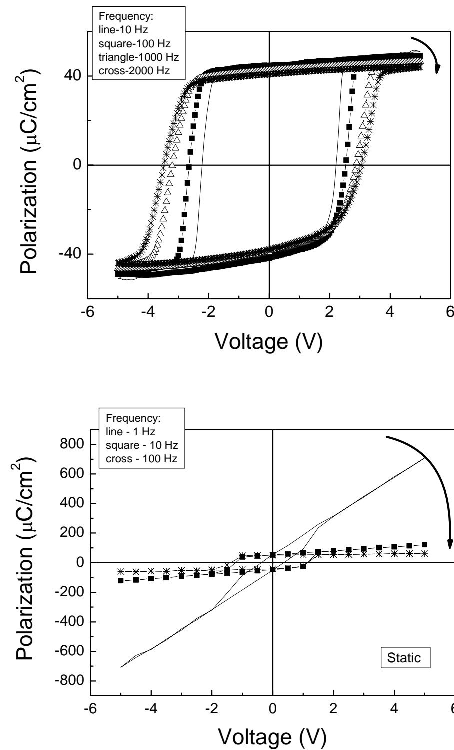

Fig. 6 Dynamic (left) and static (right) hysteresis loops obtained at different frequencies on a PZT20/80 epitaxial layer.

It can be seen that the traps bring an additive contribution to the linear term of equation (2). This is equivalent to a higher dielectric constant in the voltage range where the ferroelectric polarization is saturated. It is known that in this range the slope of the *D(E)* representation should be the dielectric constant ε. When present, the traps will lead to an apparently higher value of this quantity, value which is fast decreasing with frequency.

This theory was tested on a PZT20/80 sample of excellent epitaxial quality. The hysteresis loops obtained at different frequencies are shown in figure 6 for both dynamic and static modes.

The "dielectric constant" was calculated from the slope of the straight line in the polarization's saturation regime, as:

$$"\varepsilon" = \varepsilon_0 \varepsilon + \frac{q d w_t N_{T0}}{4 \tau V_a f} \tag{7}$$

The obtained values were represented as function of frequency, in Fig. 7, in logarithmic scale. As expected, the "dielectric constant" decreases with frequency very fast. Neglecting the $\varepsilon_0\varepsilon$ term, the frequency dependence in logarithmic scale should be linear with negative slope. This is confirmed by the graphs shown in figure 7. The differences between the values obtained from static and dynamic hysteresis loops are due to the different principles of measurements (in the static hysteresis there is a relaxation time for the polarization, while in the dynamic mode the voltage is continuously varied).

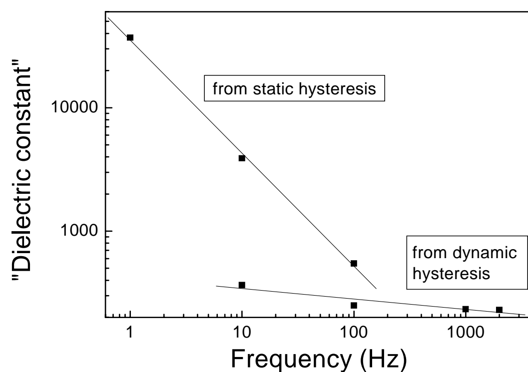

Fig. 7 The frequency dependence of the "dielectric constant" according to equation (6).

This results support the observation based on capacitance measurements that, in the low frequency range, the dielectric constant is dominated by extrinsic contributions coming from structural defects.

Before ending the discussion regarding the hysteresis loop, I have to draw the attention that the presence of a hysteresis loop in a system is not necessarily an ultimate evidence for the presence of ferroelectricity. Very often reports are published claiming ferroelectricity based on a single hysteresis loop measured at a specific frequency. It is not very difficult to show that hysteresis loop can be easily obtained, both experimentally and theoretically, on systems that have nothing to do with ferroelectricity [37,38]. For example, a back-to-back connection of two Schottky diodes with some parallel resistor-capacitance (R-C) circuit in between can give a hysteresis as shown in Fig. 8.

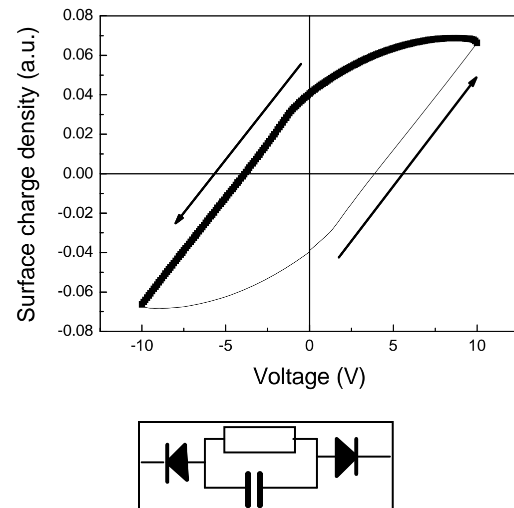

Fig. 8 The hysteresis loop obtained with the electronic circuit shown on the right side of the graphic. The circuit mimics the equivalent circuit of a MFM structure.

This result strongly supports the presence of the Schottky contacts in MFM structures. Also, it was shown theoretically that a hysteresis loop can be generated by the presence of a non-uniform distribution of traps in a semiconductor with symmetric Schottky contacts [39]. Recently, it was shown that even a banana can show a hysteresis loop [40].

In order to confirm that a material is ferroelectric or not based on hysteresis measurements we should perform these measurements at different frequencies. The polarization should be frequency-independent in the frequency range used for measurements, while other sources for hysteresis are generally strongly frequency-dependent. For comparisons, see the figure 9, showing the hysteresis measured at different frequencies on a true ferroelectric system and on the circuit presented in Fig. 8.

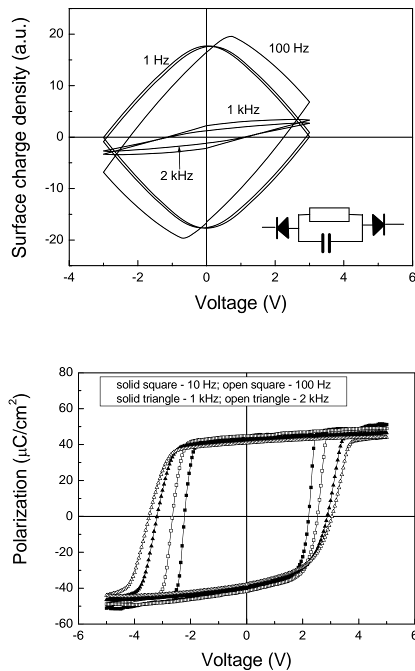

Fig. 9 Left: simulated hysteresis loop with an electronic circuit similar to the equivalent circuit of a MFM structure; Right: hysteresis loops recorded on an epitaxial PZT film.

In any case, if a hysteresis loop is obtained experimentally on a system which is not known if it is ferroelectric or not, then the presence of ferroelectricity should be confirmed by another independent method, as for example piezoelectric force microscopy (PFM), birefringence, etc.

2.3 Current

There are several conduction mechanisms which were considered to be responsible for the leakage current in ferroelectric capacitors. These can be grouped in two types [36]:

- *Interface limited.* The thermionic emission, known also as Schottky emission, and the Fowler-Nordheim tunneling are the conduction mechanisms in which the current density is directly dependent on the electrode-ferroelectric interface properties, especially the height of the potential barrier.
- *Bulk limited.* Space charge limited current (SCLC), ohmic conduction (whatever it is electronic or ionic), Pool-Frenkel emission (electric field assisted emission from the bulk traps), and hopping are conduction mechanisms that are controlled by bulk properties such as carriers mobility and concentration, traps, etc.

The dominant conduction mechanism can change, depending on the film microstructure, temperature, layer thickness, and quality of the metal-ferroelectric interface. As it was shown in the previous sections, dedicated to capacitance and hysteresis measurements, the microstructure can have a decisive influence on the magnitude of the physical quantities measured at macroscopic level. The observation remains valid also in the case of current measurements. Figure 10 shows the I-V characteristics recorded for three PZT layers, of the same composition (PZT20/80), but with different densities of structural defects. As can be seen, the highest value for the leakage current is obtained for the case of the epitaxial film free of extended structural defects (dislocations), and the lowest for the case of the polycrystalline film. This result is not surprising, considering that any structural defect can act as trapping or scattering center for the carriers injected from the electrode to the ferroelectric film. The injection is controlled by the electrode-ferroelectric interface, while the movement through the film volume is controlled by the bulk. The lower the density of the structural defects, the lower will be the influence of the bulk on the injected carrier. The carriers will have a higher mobility and a longer mean free path when the defect density is reduced. This leads to a higher value for the leakage current.

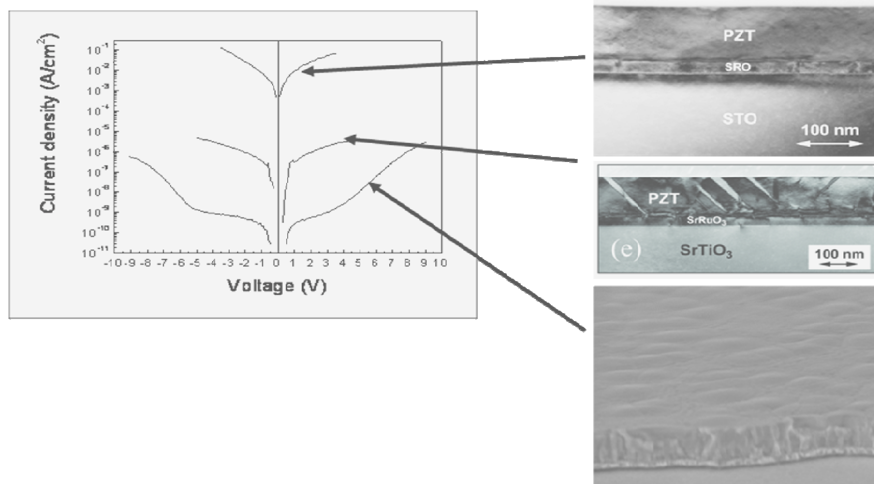

Fig. 10 The I-V characteristics for the case of three PZT layers, of the same composition (Zr/Ti=20/80) but of different crystalline qualities.

In any case, the problem of the dominant conduction mechanism at room temperature, in PZT type films, was not yet solved. Many reports claim that the leakage current is dominated by the Schottky emission, while others claim Pool-Frenkel or SCLC as dominant conduction mechanism, but no one makes the correlation with the microstructure. [41-50] We have performed a comprehensive study of the leakage current in PZT films using a batch of epitaxial samples of different thicknesses. The results of the I-V measurements performed at different temperatures and thicknesses are shown in Fig. 11.

It was observed that the magnitude of the current is only weakly dependent on the thickness in the 50 nm-270 nm range. In the case of SCLC the current density depends of thickness as $1/d^3$, with d the thickness of the ferroelectric film. If SCLC is the dominant conduction mechanisms, then the current should vary of about 600 times on the investigated thickness range, which is not the case. This result, correlated with the existing asymmetry between the negative and positive branches of the I-V characteristic, strongly suggests that the dominant conduction mechanism is interface controlled.

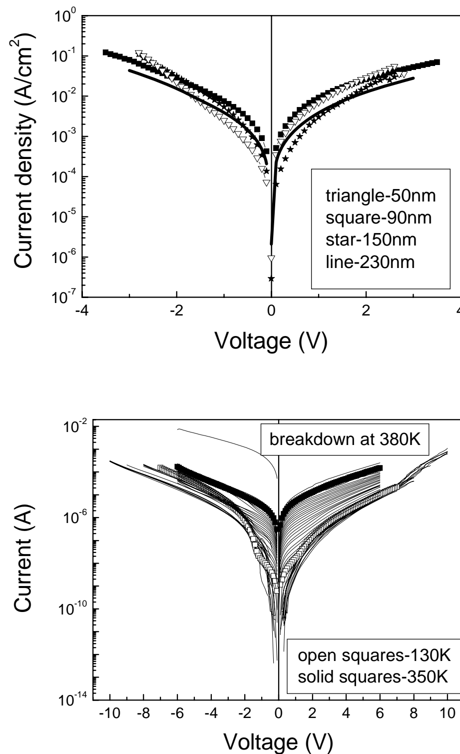

Fig. 11 Left: the thickness dependence; Right: the temperature dependence of the leakage current in case of epitaxial PZT thin films.

Therefore, we have analyzed the results of the temperature measurements considering the Schottky emission as possible conduction mechanism in the PZT capacitors [34]. We mention here that the contacts were from SRO. The use of SRO is a pre-requisite to obtain the epitaxial quality. Details about this analysis can be found elsewhere, I will only mention that the values returned for the potential barrier at the SRO-PZT interface and for the Richardson's constant were 0.12 eV and 5×10^{-7} A/cm^2K^2 respectively. Both values are far too low compared with the expected ones. The literature reports a value around 1 eV for the potential barrier, while the Richardson's constant is with about 8 orders of magnitude lower than for other materials.

The imposed conclusion is that the main conduction mechanism is not the pure thermionic (Schottky) emission and that the bulk should play also a role, as suggested by the results shown in figure 10 for different microstructures. In fact, the Schottky theory for the thermionic emission is valid if the mean free path of the injected carriers is larger than the film thickness. The mean free path can be calculated with [3]:

$$E_B \lambda = \Phi_M - \Phi_{FE} \quad (8)$$

E_B is the breakdown field, λ is the mean free path and Φ_M and Φ_{FE} are the work functions for the metal and ferroelectric, respectively. The work function difference is proportional to the potential barrier, while the value of E_B is determined experimentally to be around 50 MV/m in case of epitaxial PZT. The mean free path value was calculated to about 20 nm for a barrier of 1 eV. This value is lower than the thickness of the studied films, thus the Schottky equation for the current density must be replaced with the Simmons equation for the drift-diffusion controlled thermionic emission [51]:

$$J = 2q\left(\frac{2\pi m_{eff} kT}{h^2}\right)^{3/2} \mu E \exp\left(-\frac{q}{kT}\left(\Phi_B^0 - \sqrt{\frac{qE_m}{4\pi\varepsilon_0\varepsilon_{op}}}\right)\right) \quad (10)$$

The notations have the usual meanings. E_m is the maximum field at the Schottky contact, which is dependent on the polarization value, as shown recently. For high values of polarization the current density, in the special case of metal-ferroelectric interface, can be written as:

$$J = 2q\left(\frac{2\pi m_{eff} kT}{h^2}\right)^{3/2} \mu E \exp\left(-\frac{q}{kT}\left[\left(\Phi_B^0 - \sqrt{\frac{qP}{4\pi\varepsilon_0^2\varepsilon_{op}\varepsilon_{st}}}\right) - \sqrt{\frac{2q^2 N_{eff} V}{8\pi\varepsilon_0\varepsilon_{op} P}}\right]\right) \quad (11)$$

Two important observations can be made regarding equation (11)

1. The pre-exponential term is dependent on the mobility and the effective mass of the carriers. This can explain the low value of the "Richardson's" constant calculated by the erroneous assumption of the Schottky theory for the thermionic emission, in which the pre-exponential term is independent of field and mobility.
2. The potential barrier at zero bias Φ_B^0 is significantly reduced by a term which is dependent on the

polarization P and the static and optic dielectric constants ε_{st}, ε_{op}. This can explain the low value of the potential barrier obtained from experimental data.

The validity of the equation (11) was checked by the graphical representation of:

$$Ln\left(\frac{J}{T^{3/2}}\right) = Ln\left(2q\left(\frac{2\pi m_{eff}k}{h^2}\right)^{3/2}\mu E\right) - \frac{q}{kT}\left(\Phi_B^0 - \sqrt{\frac{qE_m}{4\pi\varepsilon_0\varepsilon_{op}}}\right) \quad (12)$$

These are shown in Fig. 12.

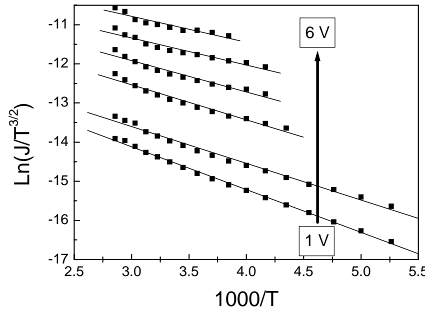

Fig. 12 The Simmons representation (12) in case of an epitaxial PZT film of 215 nm thickness.

The apparent potential barrier is determined from the slope of the Ln($J/T^{3/2}$)~$1/T$, as:

$$\Phi_{app}^0 = \Phi_B^0 - \sqrt{\frac{qE_m}{4\pi\varepsilon_0\varepsilon_{op}}} \quad (13)$$

And the pre-exponential factor from the intercept, as:

$$K(V) = 2q\left(\frac{2\pi m_{eff}k}{h^2}\right)^{3/2}\mu E(V) \quad (14)$$

Further on, from the $\Phi_{app} \sim V^{1/2}$ representation is determined the reduced potential barrier at zero bias:

$$\Phi_{red}^0 = \Phi_B^0 - \sqrt{\frac{qP}{4\pi\varepsilon_0^2\varepsilon_{op}\varepsilon_{st}}} \quad (15)$$

$\Phi_{app} \sim V^{1/2}$ representation is presented in figure 13. The intercept gives Φ_{red}^0. The obtained value is 0.13 eV. This is the reduced value due to the presence of polarization charge near the electrode interface. The true value can be calculated from (15) if the polarization and dielectric constants values are known. For the present case these are: 100 μC/cm^2, 80 and 6.5 respectively [52]. Replacing the numbers in equation (15), then a value of 0.72 eV is obtained for Φ_B^0. This is much closer to the expected value of 1 eV.

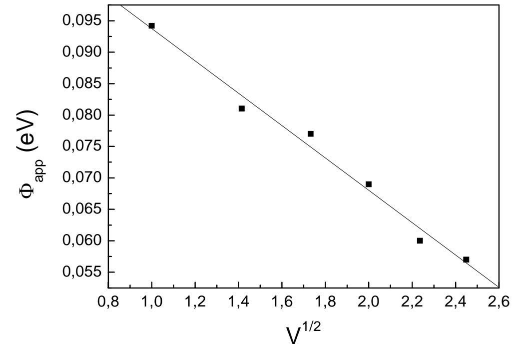

Fig. 13 The $\Phi_{app} \sim V^{1/2}$ representation, where Φ_{app} is given by equation (13)

The voltage dependence of the pre-exponential factor K(V) defined by equation (14) is presented in figure 14.

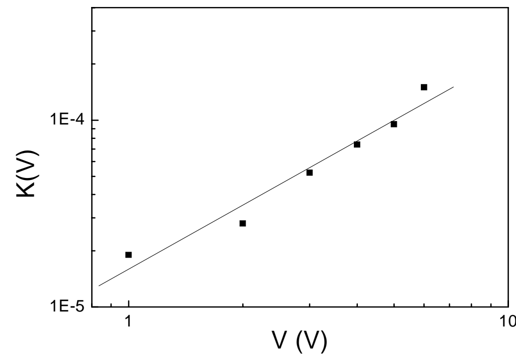

Fig. 14 The voltage dependence of the pre-exponential factor K(V) defined by equation (14).

The dependence is approximately linear, with a confidence factor higher than 0.99. This result suggests that the electric field in equation (14) should be proportional with voltage, considering that the carrier mobility is not dependent on the electric field.

The analysis of the current data leads to the conclusion that the electric field inside the MFM structure is strongly non-uniform. There is a non-linear, position dependent, electric field in the depleted region of the Schottky metal-ferroelectric contact, which is dependent on the polarization charge, and there is a small, linear electric field in the volume of the film. Here linearity or non-linearity refers to the voltage dependence of the electric field.

The equations for the two fields are [31,32]:

$$E_m = \sqrt{\frac{2qN_{eff}(V + V_{bi}')}{\varepsilon_0\varepsilon_{st}}} + \frac{P}{\varepsilon_0\varepsilon_{st}} \quad (16)$$

This is the maximum electric field at the electrode interface.

$$E = \frac{V}{d} \quad (17)$$

This is the electric field inside the film, in the volume between the two depleted regions located near electrode interfaces.

The schematic band diagram for the MFM structure is presented in figure 15 for a p-type conductivity in the ferroelectric material.

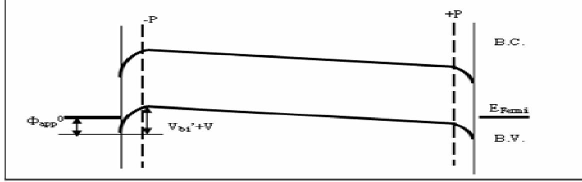

Fig. 15 The band diagram for a MFM structure. BC is for conduction band, BV is for valance band, P for polarization, V_{bi}' is the built-in potential with the effect of polarization included, and V is the applied voltage.

This model does not contradict the results and conclusions drawn from capacitance and hysteresis measurements. What it can be said in the case of MFM structures based on epitaxial PZT type materials is that:

- They can be modeled as two back-to-back Schottky diodes with a leaky capacitor in between;
- The PZT type materials behaves more like wide band gap semiconductors than pure insulators, at least for compositions in the tetragonal phase
- The MFM structure is only partly depleted if the thickness of the film is larger than about 20 nm

Of course, this behavior can change dramatically in polycrystalline films, but the PZT material itself remains with a semiconductor behavior. What it is changing is the weight of the extrinsic contributions, which become dominant compared to the intrinsic ones. The main effect is that, most probably, the grain boundaries and other structural defects will mask the contribution from the volume of the grains. On the other hand, they can hidden the contribution of the electrode interfaces, so that the volume overtakes the control of the macroscopic properties in the case of the very fine grained films.

3. Recent topics in the field of ferroelectric structures

3.1 Conduction mechanisms in other ferroelectric materials

It is interesting to study the leakage current in other materials with perovskite structure very similar to that of tetragonal PZT. One of these materials is $BaTiO_3$ (BTO). Practically, the only difference is that the Pb atom is replaced with Ba one. This is, apparently, a minor change but, in reality is producing strong differences. As mentioned in the introduction, the differences are related to the different behavior of the Pb-O bound compared to Ba-O bound.

A careful analysis of the capacitance and hysteresis results shows that the BTO films behaves as fully depleted, and that the BTO is closer to an ideal insulator than PZT. The comparative C-V characteristics and hysteresis loops are shown in figure 16.

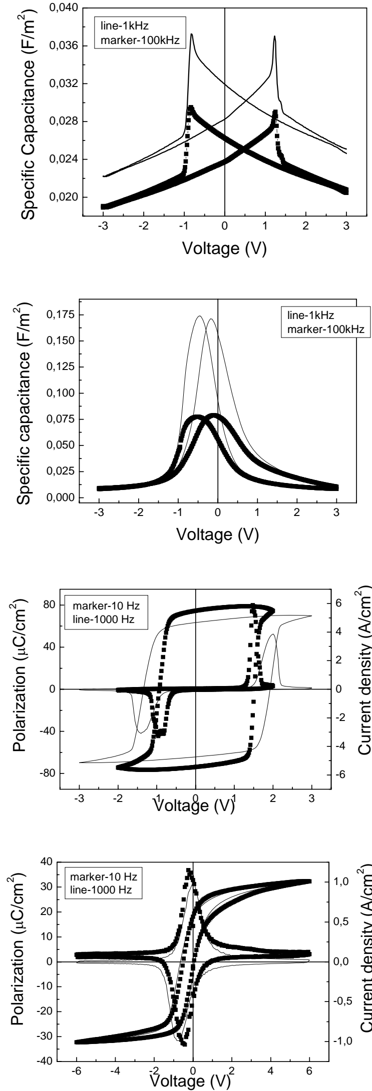

Fig. 16 Left hand: C-V characteristic and hysteresis loop in case of an epitaxial PZT40/60 film with tetragonal structure; Right hand: C-V characteristic and hysteresis loop for an epitaxial BTO film. PZT films were grown at MPI Halle, while the BTO films were delivered by the group of Prof. Kohlstedt from Forschungszentrum Jülich, Germany.

The most significant difference was observed in the case of the leakage current. In BTO the leakage current is with several orders of magnitude lower than in PZT, as shown in figure 17. Further on, the detailed analysis of the thickness and temperature dependencies of the I-V

characteristics suggests that the conduction mechanism is very different in BTO compared to PZT. The most striking result was that the magnitude of the leakage current is decreasing with the film thickness, as shown in figure 18. This behavior is opposite to that encountered in the case of the PZT films. The only conduction mechanisms showing such a thickness dependence is the hopping conduction [53-55].

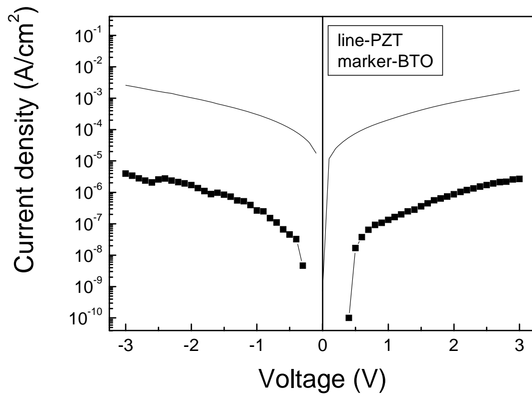

Fig. 17 Comparative I-V characteristics for tetragonal PZT and BTO films of epitaxial quality.

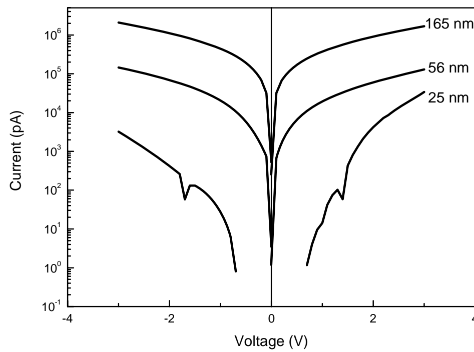

Fig. 18 I-V characteristics for tetragonal, epitaxial BTO films with different thicknesses.

The analysis of the temperature measurements, correlated with the voltage dependence, hints towards a small polaron hopping as the dominant conduction mechanism in epitaxial BTO thin films, [56] with the amendment that the injection of charge carriers is still controlled by the interfaces. The following equation is suggested for the current density:

$$J = F_1(E)\exp\left(-\frac{q}{kT}\left(\left(\Phi_B^0 + W_a\right) - \sqrt{\frac{qE}{4\pi\varepsilon_0\varepsilon_{op}}}\right)\right) \quad (18)$$

The equation is similar to the Simmons equation (10). The pre-exponential factor should depend on mobility. W_a is the hopping barriers, and the electric field is constant and equal to V/d, where d is the film thickness. Of course, this equation does not evidence the thickness dependence observed experimentally. The thickness dependence in case of doping can be explained through the density of the structural defects, which may change with thickness and which can affect the height of the potential barrier by pinning the Fermi level.

Serial versus parallel capacitor model in case of ferroelectric multilayers.

Ferroelectric multilayers and supper-lattices are increasingly studied in the last years due to their potential to obtain enhanced characteristics and even new properties [57-60]. One observed phenomena is the increase of the dielectric constant with decreasing the thickness of the component layers in the multilayers/super-lattices. This was explained through the Maxwell-Wagner relaxation, which is a phenomenon occurring in multilayers or composites formed of materials with very different values for the electric conductivity, for example a dielectric and a metal [61]. However, in ferroelectric multilayers made of materials with similar structures, like PZT with different Zr/Ti ratio or (Ba,Sr)TiO_3 (BST) with different Sr content, it is hard to believe that the electric conductivity from one layer to the other varies with orders of magnitude. Therefore, there should be another explanation for the observed increase of the dielectric constant. Recently I have suggested that this increase can be due to the presence of either an interfacial polarization, or to the presence of some interface charges bringing an additive contribution to the overall capacitance of the multilayer [62].

This brings into light the problem of the equivalent circuit in the case of a ferroelectric multilayer. The custom is to use a serial connection of capacitors in order to describe the multilayer, but in this case the equivalent capacitance will be smaller than the capacitance of any of the component layers, thus the serial model cannot explain an increase of the capacitance as the number of layers increases (see figure 19).

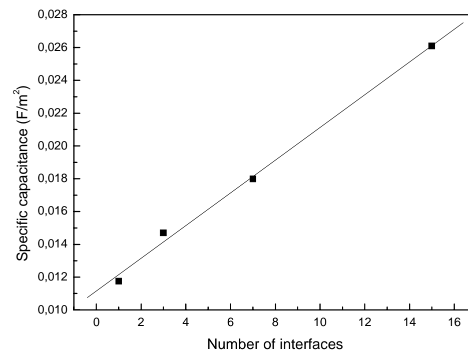

Fig. 19 The dependence of the specific capacitance on the number of interfaces in the case of an epitaxial multilayer made from PZT80/20 and PZT20/80.

The calculations performed for a bi-layer with a surface charge density σ located at the interface between layers have lead to the following expression for the equivalent capacitance:

$$C_\sigma = \frac{\varepsilon_0}{L}\left[\frac{1}{\varepsilon_1+\varepsilon_2}\left(\varepsilon_1\varepsilon_2 * + \varepsilon_2\varepsilon_1 *\right)\right] + \frac{d}{dV}\left(\frac{1}{2}\sigma\right) = C + \frac{d}{dV}\left(\frac{1}{2}\sigma\right) \quad (19)$$

Here ε_1 and ε_2 are the dielectric constants of the two materials when the ferroelectric polarization is saturated, while ε_1* and ε_2* are the dielectric constant including the contribution of the $\frac{1}{\varepsilon_0}\frac{\partial P_S}{\partial E}$ term. L is the thickness of the bi-layer. It was assumed that the dielectric constants are of close values, in order to simplify the calculations for the image charges induced by the interface charge σ on the two electrodes.

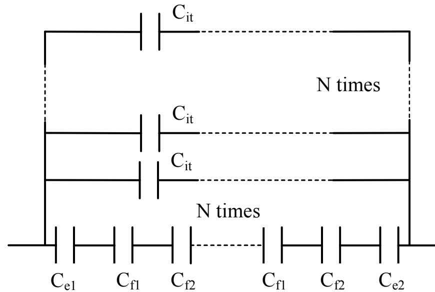

Fig. 20 The equivalent circuit for a ferroelectric multilayer in which each interface carries a surface charge σ. In case of N interfaces, this is equivalent to the parallel connection of N interface capacitances to the standard serial circuit. C_{e1} and C_{e2} refer to the two capacitances related to the presence of the Schottky contacts, while C_{fi} refers to the capacitance of the i-th ferroelectric layer.

Returning to equation (19) it can be observed that this turns to the standard serial connection if σ is zero. When σ is non-zero, then the image charges bring an additive contribution to the capacity which can be modeled as a parallel capacitor added to the standard serial connection. The equivalent circuit in this case is shown in figure 20.

The conclusion is that the acceptance or the rejection of a specific equivalent circuit should be made after a critical analysis of the experimental results. The dogmatic affirmation that only serial model must be used in case of ferroelectric layers is not valid when there are interfaces carrying charges.

3.3 Coexistence of ferroelectricity and antiferroelectricity in ferroelectric materials and multilayers.

The coexistence of ferroelectricity and antiferroelectricity in $PbZrO_3$ (PZO) is an old hypothesis, signaled from the moment of the discovery of the antiferroelectric (AFE) behavior in PZO [63,64]. However, the controversy could not be solved until last year because it requires single-crystal like samples. It was possible to obtain such samples by PLD growing of epitaxial PZO films. Moreover, by changing the buffer layer between the $SrTiO_3$ substrate and the PZO film it was possible to obtain layers with different orientations. In this way it was possible to clearly evidence the presence of the ferroelectric (FE) behavior in PZO [65]. The dominance of the AFE or FE behavior is temperature dependent, but on the temperature domain on which AFE and FE coexist a triple hysteresis loop is obtained, similar to that presented in figure 21.

It was also predicted theoretically that AFE behavior should be obtained in certain conditions in multilayers made from ferroelectric components [66-68]. This case is possible when a certain AFE coupling is present at the separation interface between component layers, and when the layers have comparable thickness. The AFE behavior in FE multilayers was rarely reported in the literature, [69] and very often its presence is contested based on the model of "pinched" hysteresis [70] . This model says that double hysteresis-like loops, similar to those obtained in the case of AFE materials, can be present even in FE layers if there are internal electric fields pinning ferroelectric domains. The electric field may develop around charged defects. However, the "pinched" hysteresis returns to a normal FE hysteresis after a few cycles, while in the case of the AFE coupling at the interface the AFE behavior is stable although the shape of the loop may change do to the redistribution of the charged defects during the hysteresis measurements. Recently, a double hysteresis loop suggesting an AFE-like behavior was obtained on PZT-$BiFeO_3$ multilayers. This is presented in figure 22. The AFE behavior remains after as much as 10^5 switching cycles, suggesting that it is not a "pinched" hysteresis.

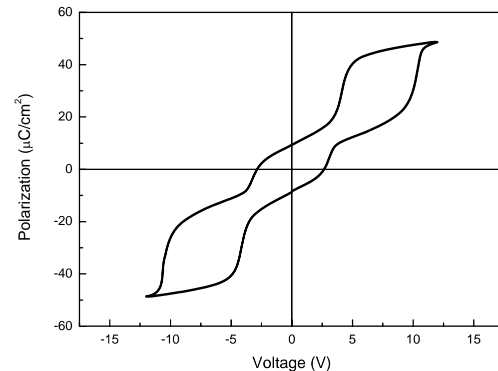

Fig. 21 Triple hysteresis loop obtained in the case of an epitaxial PZO film.

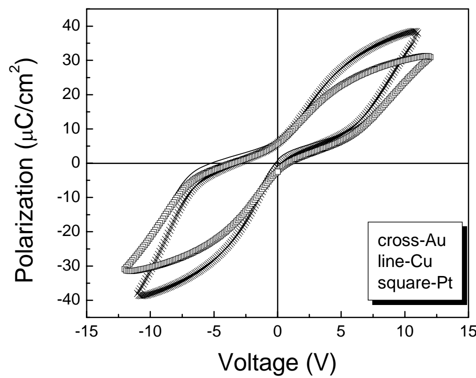

Fig. 22 The hysteresis loops obtained in the case of a PZT-BiFeO$_3$ multilayer with different top electrodes.

4. Conclusions

A critical analysis of the main measurements performed to investigate the electrical properties of the ferroelectric capacitors was presented. It was shown that the results should be carefully examined, in close correlation with the potential theoretical models, in order to avoid wrong interpretation. An increased attention should be given to details such as microstructure, electrode interfaces, or separation interfaces between component layers in multilayers.

Some recent results were presented at the end, supporting the idea that the field of ferroelectrics is still very interesting for research and that many new results and phenomena can be obtained in the future.

Acknowledgment

The author wish to thank to the following persons for helping him with samples, for providing him the opportunity to perform measurements, and for the useful discussions: PhD student Lisca Marian, Dr. Stancu Viorica, Dragoi Cristina from NIMP, Magurele, Romania; Dr. Marin Alexe, Dr. Ionela Vrejoiu, Dr. Ksenia Boldyreva, Dr. Gwenael LeRhun, Prof. Dietrich Hesse, Prof. Ulrich Goesele from MPI-Halle, Germany; Dr. Y. H. Chu, National Chiao Tung University, Taiwan; Prof. R. Ramesh, University of California, Berkeley, USA; Dr. Andrei Petraru, Institute of Solid State Research, Forschungszentrum Jülich, Germany.

The polycrystalline samples, including PZT-BiFeO$_3$ multilayers were prepared at NIMP, while the epitaxial samples and multilayers were prepared mainly at MPI-Halle, Germany, except the BaTiO$_3$ film, which were prepared at Forschungszentrum Jülich, Germany.

References

[1] K. Uchino, Ferroelectric Devices, (Marcel Dekker, New York, 2000).
[2] A. M. Glass and M. E. Lines, Principles and Applications of Ferroelectrics and Related Materials (Clarendon Press, Oxford, 1977).
[3] J. F. Scott, Ferroelectric Memories, in Advanced Microelectronics series edited by K. Itoh and T. Sakurai (Springer-Verlag, Berlin, Heidelberg, 2000).
[4] J. F. Scott, Ferroelectrics Review **1**, 1(1998).
[5] M. Dawber, K. M. Rabe, J. F. Scott, Rev. Mod. Phys. **77**, 1083 (2005).
[6] A.K. Tagantsev, V.O. Sherman, K. F. Astafiev, J. Venkatesh & N. Setter, Journal of Electroceramics, **11**, 5–66, (2003).
[7] J. F. Scott, Science **315**, 954 (2007).
[8] N. Izyumskaya, Y. I. Alivov, S. J. Cho, and H. Morkoc, H. Lee, Y. S. Kang, Critical Reviews in Solid State and Materials Sciences **32**, 111 (2007).
[9] N. Setter, D. Damjanovic, L. Eng, G. Fox, S. Gevorgian, S. Hong, A. Kingon, H. Kohlstedt, N. Y. Park, G. B. Stephenson, I. Stolitchnov, A. K. Taganstev, D. V. Taylor, T. Yamada, S. Streiffer, J. Appl. Phys. **100**, 051606 (2006).
[10] J. Schwarzkopf, R. Fornari, Progress in Crystal Growth and Characterization of Materials **52**, 159-212 (2006).
[11] S. K. Dey, J. J. Lee, P. Alluri, Jpn. J. Appl. Phys. **34**, 3142 (1995).
[12] J. F. Scott, Ann. Rev. Mater. Sci. 28, 79 (1998).
[13] J. F. Scott, Jap. J. Appl. Phys. 38, 2272 (1999).
[14] U. Ellerkmann, R. Liedtke, U. Boettger, R. Waser, Appl. Phys. Lett. **85**, 4708 (2004).
[15] Ho Jin Cho, Hyeong Joon Kim, Appl. Phys. Lett. **72**, 786 (1998).
[16] N. Sai, K. M. Rabe, D. Vanderbilt, Phys. Rev. **B 66**, 104108 (2002) .
[17] M. Klee, R. Eusemann, R. Waser, W. Brand, H. van Haal, J. Appl. Phys. **72**, 1566 (1992).
[18] T. Oikawa, M. Aratani, K. Funakubo, K. Saito, M. Mizuhira, J. Appl. Phys. **95**, 3111 (2004).
[19] S. Yokoyama, Y. Honda, H. Morioka, S. Okamotot, H. Funakubo, T. Iijima, H. Matsuda, K. Saito, T. Yamamoto, H. Okino, O. Sakata, S. Kimura, J. Appl. Phys. **98**, 94106 (2005).
[20] C. M. Foster, G. R. Bai, R. Csencsits, J. Vetrone, R. Jammy, L. A. Wills, E. Carr, J. Amanao, J. Appl. Phys. **81**, 2349 (1997).
[21] D. Vanderbilt, R. D. King-Smith, Phys. Rev. B **48**, 4442 (1993).
[22] A.M. Bratkovsky, A.P. Levanyuk, Appl. Phys. Lett. **89**, 253108 (2006).
[23] R. E. Cohen, Nature **358**, 136 (1992).
[24] I. Vrejoiu, G. Le Rhun, L. Pintilie, D. Hesse, M. Alexe, U. Gösele, Advanced Materials **18**, 1657 (2006).

[25] I. Vrejoiu, G. Le Rhun, N. D. Zakharov, D. Hesse, L. Pintilie, M. Alexe, Philosophical Magazine **86**, 4477 (2006).
[26] I. Vrejoiu, Y. Zhu, G. Le Rhun, M. A. Schubert, D. Hesse, M. Alexe, Appl. Phys. Lett. **90**, 072909 (2007).
[27] J. A. Sanjurjo, E. Lopez-Cruz, and G. Burns, Phys. Rev. B **28**, 7260 (1983).
[28] I. Stolichnov, A. Tagantsev, J. Appl. Phys. **84**, 3216 (1998).
[29] J. D. Baniecki, T. Shioga, K. Kurihara, and N. Kamehara, J. Appl. Phys. **94**, 6741 (2003)
[30] J. Robertson, J. Appl. Phys. **93**, 1054 (2003)
[31] L. Pintilie M. Alexe, J. Appl. Phys. **98**, 124103 (2005).
[32] L. Pintilie, M. Alexe, J. Appl. Phys. **98**, 124103 (2005); L. Pintilie, I. Boerasu, M. J. M. Gomes, T. Zhao, R. Ramesh, M. Alexe, J. Appl. Phys. **98**, 124104 (2005).
[33] I. Boerasu, L. Pintilie, M. Pereira, M. I. Vasilevskiy, M. J. M. Gomes, J. App. Phys. **93**, 4776 (2003).
[34] L. Pintilie, I. Vrejoiu, D. Hesse, G. LeRhun, and M. Alexe, Phys. Rev. B **75**, 104103 (2007).
[35] D. K. Schroeder, Semiconductor material and device characterization, (Wiley-Interscience, New York, 1998).
[36] S. M. Sze, Physics of Semiconductor Devices, 2nd ed. (John Wiley & Sons, 1981), Chaps 7 and 10.
[37] T. Tsurumi, T. Harigai, D. Tanaka, S. M. Nam, H. Kakemoto, S. Wada, K. Saito. Appl. Phys. Lett. **85**, 5016 (2004).
[38] R. Waser, O. Lohse, Integr. Ferroelectrics **21**, 27 (1998).
[39] L. Pintilie, M. Alexe, Appl. Phys. Lett. **87**, 112903 (2005).
[40] J. F. Scott, J. Phys.: Condens. Matter **20**, 021001 (2008).
[41] T. Mihara and H. Watanabe, Jpn. J. Appl. Phys. **34**, 5664 (1995); Jpn. J. Appl. Phys. **34**, 5674 (1995).
[42] P. W. Boom, R. M. Wolf, J. F. M. Cillessen, and M. P. C. M. Krijn, Phys. Rev. Lett. **73**, 2107 (1994).
[43] J. C. Shin, J. Park, C. S. Hwang, and H. J. Kim, J. Appl. Phys. **86**, 506, (1999).
[44] C. Hwang, B. T. Lee, C. S. Kang, K. H. Lee, H. Cho, H. Hideki, W. D. Kim, S. I. Lee, and M. Y. Lee, J. Appl. Phys. **85**, 287 (1999).
[45] Y. S. Yang, S. J. Lee, S. H. Kim, B. G. Chae, and M. S. Jang, J. Appl. Phys. **84**, 5005 (1998).
[46] B. Nagarajan, S. Aggarwal, and R. Ramesh, J. Appl. Phys. **90**, 375 (2001).
[47] S. Bhattacharyya, A. Laha, and S. B. Krupanidhi, J. Appl. Phys. **91**, 4543 (2002).
[48] H. Schroeder, S. Schmitz, and P. Meuffels, Appl. Phys. Lett. **82**, 781 (2003).
[49] B. Chen, H. Yang, J. Miao, L. Zhao, L. X. Cao, B. Xu, X. G. Qiu, and B. R. Zhao, J. Appl. Phys. **97**, 024106 (2005).
[50] P. Zubko, D. J. Jung, and J. F. Scott, J. Appl. Phys. **100**, 114113 (2006).
[51] J. G. Simmons, Phys. Rev. Lett. **15**, 967 (1965)
[52] L. Pintilie, I. Vrejoiu, D. Hesse, G. LeRhun, and M. Alexe, Phys. Rev. B **75**, 224113 (2007).
[53] J Rybickiy, A Rybickay, S Feliziani and M Chybicki, J. Phys: Condens. Matter. **8**, 2089 (1996).
[54] M. L. Knotek, M. Pollak, T. M. Donovan, H. Kurtzman, Phys. Rev. Lett. **30**, 853 (1973).
[55] M.A. Angadi, S. M. Shivaprasad, J. Mater. Sci. Lett. **5**, 405 (1986).
[56] U. Boettger and V. Bryskin, "Hopping Conduction is Solids", Akademie Verlag, Berlin, 1985, pp. 55
[57]H. M. Christen, E. D. Specht, S. Silliman, and K. S. Harshavardhan, Phys. Rev. B **68**, 020101 (2003).
[58] C. Bungaro and K. M. Rabe, Phys. Rev. B **69**, 184101 (2004).
[59] F. M. Pontes, E. Longo, J. A. Varela, and E. R. Leite, Appl. Phys. Lett. **84**, 5470 (2004).
[60] H. N. Lee, H. M. Christen, M. F. Chisholm, C. M. Rouleau, D. H. Lowndes, Nature **433**, 395 (2005).
[61] M. H. Corbett, R. M. Bowman, D. T. Ford, and J. M. Gregg, Appl. Phys. Lett. **79**, 815 (2001).
[62] L. Pintilie, K. Boldyreva, M. Alexe and D. Hesse, New J. Phys. 10, 013003 (2008) .
[63] F. Jona, G. Shirane, F. Mazzi, and R. Pepinsky, Phys. Rev. **105**, 849 (1957).
[64] X. Dai, J-F. Li, and D. Viehland, Phys. Rev. B **51**, 2651 (1995).
[65] L. Pintilie, K. Boldyreva, M. Alexe, and D. Hesse, J. Appl. Phys. **103**, 024101 (2008).
[66] H. M. Christen, E. D. Specht, S. S. Silliman, and K. S. Harshavardhan, Phys. Rev. Lett. **68**, 020101(R) (2003).
[67] L. -Hock Ong, J. Osman, and D. R. Tilley, Phys. Rev. B **65**, 134108 (2002).
[68] S. Hao, G. Zhou, X. Wang, J. Wu, W. Duan, and B.-Lin Gu, Appl. Phys. Lett. **86**, 232903 (2005) .
[69] R. Ranjith and S. B. Krupanidhi, Appl. Phys. Lett. **91**, 082907 (2007).
[70] G. Robert, D. Damjanovic, and N. Setter, Appl. Phys. Lett. **77**, 4413 (2000).

Corresponding author: pintilie@infim.ro